LSR defines cell corners for tricellular tight junction formation in epithelial cells

Sayuri Masuda[1,2], Yukako Oda[1], Hiroyuki Sasaki[3], Junichi Ikenouchi[4,5], Tomohito Higashi[1], Masaya Akashi[1], Eiichiro Nishi[6] and Mikio Furuse[1,*]

[1]Division of Cell Biology, Department of Physiology and Cell Biology, Kobe University Graduate School of Medicine, Kobe 650-0017, Japan
[2]Department of Cell Biology, Graduate School of Medicine, Kyoto University, Kyoto 606-8501, Japan
[3]Department of Molecular and Cell Biology, Institute of DNA Medicine, Jikei University School of Medicine, Tokyo 105-8461, Japan
[4]Department of Synthetic Chemistry and Biological Chemistry, Graduate School of Engineering, Kyoto University, Kyoto 615-8510, Japan
[5]Precursory Research for Embryonic Science and Technology (PRESTO), Japan Science and Technology Agency, Saitama 332-0012, Japan
[6]Department of Cardiovascular Medicine, Graduate School of Medicine, Kyoto University, Kyoto 606-8507, Japan
*Author for correspondence (furuse@med.kobe-u.ac.jp)

Accepted 18 October 2010
Journal of Cell Science 124, 548-555

doi:10.1242/jcs.072058

Summary

Epithelial cell contacts consist of not only bicellular contacts but also tricellular contacts, where the corners of three cells meet. At tricellular contacts, tight junctions (TJs) generate specialized structures termed tricellular TJs (tTJs) to seal the intercellular space. Tricellulin is the only known molecular component of tTJs and is involved in the formation of tTJs, as well as in the normal epithelial barrier function. However, the detailed molecular mechanism of how tTJs are formed and maintained remains elusive. Using a localization-based expression cloning method, we identified a novel tTJ-associated protein known as lipolysis-stimulated lipoprotein receptor (LSR). Upon LSR knockdown in epithelial cells, tTJ formation was affected and the epithelial barrier function was diminished. Tricellulin accumulation at the tricellular contacts was also diminished in these cells. By contrast, LSR still accumulated at the tricellular contacts upon tricellulin knockdown. Analyses of deletion mutants revealed that the cytoplasmic domain of LSR was responsible for the recruitment of tricellulin. On the basis of these observations, we propose that LSR defines tricellular contacts in epithelial cellular sheets by acting as a landmark to recruit tricellulin for tTJ formation.

Key words: Tight junction, Tricellular contact, Tricellulin, LSR

Introduction

Tight junctions (TJs) restrict and regulate the free diffusion of solutes through the paracellular pathway in epithelial cell types and contribute to the establishment of distinct fluid compartments within the body (Furuse and Tsukita, 2006; Schneeberger and Lynch, 2004; Van Itallie and Anderson, 2006). In ultrathin section electron microscopy, TJs are visualized as focal attachments of adjacent cell membranes that exclude the intercellular gap (Farquhar and Palade, 1963). In freeze-fracture electron microscopy, TJs appear as anastomosing linear fibrils or chains of particles, which are termed TJ strands (Staehelin et al., 1969). Each TJ strand coincides with a focal attachment between adjacent plasma membranes, forming the functional elements of TJs (Staehelin, 1973). Among the TJ-associated integral membrane proteins, claudins, which comprise a multigene family, are the major structural and functional constituents of TJ strands and are directly involved in the barrier function of TJs (Angelow et al., 2008; Furuse and Tsukita, 2006; Schneeberger and Lynch, 2004; Van Itallie and Anderson, 2006).

TJs are generally thought to work as barriers by circumscribing individual cells and sealing the intercellular space between adjacent cells (bicellular TJs; bTJs). However, more precisely, the narrow extracellular space at tricellular contacts, formed by the joining of three cells, should also be considered for sufficient sealing of the intercellular space throughout the cellular sheet. Close inspections, by freeze-fracture replica electron microscopy, have identified specialized structures at tricellular contacts, designated tricellular TJs (tTJs) (Friend and Gilula, 1972; Ikenouchi et al., 2005; Staehelin, 1973; Staehelin et al., 1969; Wade and Karnovsky, 1974; Walker et al., 1985). In freeze-fracture replicas, the belt of bTJs is not continuous at tricellular contacts, and the most apical elements of the TJ strands in bTJs from both sides join and turn to extend in the basal direction, attaching to one another. These TJ strands, termed the central sealing elements (Staehelin, 1973), are connected by short TJ strands extending from bTJs to form tTJs. Consequently, three sets of the central sealing elements attach to form a very narrow tube in the extracellular space at the center of each tricellular contact, and this structure is thought to impede the diffusion of solutes (Staehelin, 1973). However, the mechanism underlying the definition of tricellular contacts followed by tTJ formation is totally unknown.

Previously, tricellulin has been identified as the first molecular component of tTJs (Ikenouchi et al., 2005) and as a causative gene underlying familial deafness (Riazuddin et al., 2006). Tricellulin is an ~65-kDa integral membrane protein with four transmembrane domains and shows structural similarity to occludin, another TJ-associated membrane protein. The ELL domain in the C-terminal cytoplasmic region of tricellulin is particularly conserved relative to that of occludin (Ikenouchi et al., 2005; Li et al., 2005), whereas the long N-terminal cytoplasmic region of tricellulin is unique. Tricellulin is expressed in various epithelial cell types and is concentrated in the central sealing elements of tTJs (Ikenouchi et al., 2005). When tricellulin expression is suppressed in cultured epithelial cells, tTJ formation is affected and the barrier function

Journal of Cell Science

of the cellular sheet is compromised (Ikenouchi et al., 2005). Conversely, overexpression of tricellulin increases the barrier towards ions and larger solutes (Krug et al., 2009). Furthermore, exogenous tricellulin is colocalized with claudin-based TJ strands reconstituted in claudin-1-overexpressing mouse L fibroblasts. In these cells, the frequency of the TJ strand crosslinks is increased compared with that in L cells expressing claudin-1 but not tricellulin (Ikenouchi et al., 2008). Although these observations indicate a crucial role for tricellulin in tTJ formation, the molecular mechanism underlying its action is totally unknown. One of the important points to be clarified is how tricellulin is concentrated into tricellular contacts to generate tTJs. RNA interference (RNAi)-mediated suppression of occludin in cultured epithelial cells substantially increases the amount of tricellulin within bTJs, implying that tricellulin is excluded from bTJs by occludin (Ikenouchi et al., 2008). However, the factor that recruits tricellulin to tricellular contacts is unknown. Clarification of the mechanism behind tTJ formation will provide not only a new understanding of the barrier functions of epithelia but also novel insights into how polygonal epithelial cells recognize and manage cell corners within the cellular sheet.

Here, we identify lipolysis-stimulated lipoprotein receptor (LSR) as a novel molecular component of tTJs. We show that LSR recognizes the cell corners in epithelial cell sheets and defines tricellular contacts as landmarks to recruit tricellulin for tTJ formation.

Results

LSR is a novel component of tTJs

To investigate the molecular mechanism of tTJ formation, we attempted to identify novel molecular components of tTJs by localization-based expression cloning in Madin–Darby canine kidney (MDCK) cells utilizing retrovirus-based cDNA–GFP (green fluorescent protein) fusion libraries (Matsuda et al., 2008; Misawa et al., 2000; Nishimura et al., 2002). During screening with a T84 human colon-carcinoma-cell-derived cDNA library, we obtained MDCK cells showing GFP fusion protein accumulation at tricellular contacts (Fig. 1A). Cell cloning, followed by genomic PCR amplification, revealed that the cDNA in the fusion protein encoded amino acids 1–474 of human LSR, which has been cloned and studied as a receptor for triacylglyceride-rich lipoproteins (Yen et al., 1999). Human LSR comprises 581 amino acids and contains an extracellular Ig domain, a transmembrane domain and a cytoplasmic domain (Fig. 1B). We cloned the full-length mouse LSR cDNA, which encoded 575 amino acids, and confirmed that exogenous GFP-tagged mouse LSR was predominantly localized at tricellular contacts in mouse EpH4 epithelial cells (data not shown).

To examine the subcellular localization of endogenous LSR, we generated a rabbit polyclonal antibody against the cytoplasmic region of mouse LSR. Triple immunofluorescence staining of EpH4 cells with anti-LSR polyclonal antibodies, anti-tricellulin monoclonal antibodies and anti-ZO-1 (zona occludens 1) monoclonal antibodies, revealed that LSR had a dot-like staining, which colocalized with the tricellulin staining at the crossing points of the ZO-1 staining, although the staining intensity of LSR varied, depending on location (Fig. 1C). This indicated that endogenous LSR is localized at the tricellular contacts of epithelial cells. Furthermore, double immunofluorescence staining of frozen sections of various mouse epithelial tissues, with anti-LSR polyclonal antibodies and anti-occludin monoclonal antibodies, revealed that LSR was localized at tricellular contacts in vivo (Fig. 1D; supplementary material Fig. S1). The extent of the LSR accumulation at tricellular contacts varied among cell types. For example, LSR was highly concentrated into tricellular contacts in the epididymis, whereas large amounts of LSR were also detected throughout the lateral membranes in the small intestine and liver. Next, we examined the precise localization of LSR in EpH4 cells by immuno-freeze-fracture replica electron microscopy. LSR was concentrated at tTJs, especially along the central sealing elements (Fig. 1E). Taken together, these results indicate that LSR is a novel component of tTJs.

LSR assembles into cell–cell contacts

Given that LSR has an Ig domain, which is often present in cell adhesion molecules, we examined whether LSR itself assembles into cell–cell contacts. When cell-adhesion-deficient mouse L fibroblasts overexpressing LSR were co-cultured with parental L cells, exogenous LSR assembled as dots or short lines around the cell borders between LSR-expressing L cells (Fig. 2A). To evaluate further the manner of this assembly of LSR, we established two L transfectants expressing GFP-tagged LSR (GFP–LSR) and hemagglutinin (HA)-tagged LSR (HA–LSR), respectively. These cells were co-cultured, and the localizations of GFP–LSR and HA–LSR were observed by double immunofluorescence microscopy. Colocalization of GFP–LSR and HA–LSR was often observed (Fig. 2B; supplementary material Fig. S2), implying that these regions comprised cell–cell contacts between GFP–LSR-expressing L cells and HA–LSR-expressing L cells. These findings indicate that LSR has the ability to assemble into regions defining cell–cell contacts. However, LSR accumulation was also observed in single LSR-expressing L cells that were surrounded by parental L cells, although we could not evaluate whether it occurred at cell–cell contacts (Fig. 2C). It is unknown whether the manner of the assembly of LSR at cell–cell contacts is homophilic or heterophilic.

RNAi-mediated suppression of LSR affects tTJ formation, epithelial barrier function and the localization of tricellulin at tTJs

To investigate the function of LSR in tTJ formation, we established EpH4 clones with a stable short-hairpin RNA (shRNA)-mediated suppression of LSR expression (LSR-knockdown cells). The expression of LSR, which in western blotting analyses showed multiple bands of approximately 55 and 70 kDa in parental EpH4 cells, was suppressed to only trace amounts in LSR-knockdown cells (Fig. 3A). Immunofluorescence staining of occludin, a marker of TJs, revealed that tTJ formation was affected in LSR-knockdown cells. Specifically, the linkage of occludin staining at tricellular contacts appeared to be incomplete in subconfluent LSR-knockdown cells compared with that in normal cells, and abnormal accumulation of occludin was often observed in these regions (Fig. 3B; supplementary material Fig. S3). This phenotype is similar to that of tricellulin-knockdown EpH4 cells (Ikenouchi et al., 2005) and was rescued by re-expression of HA-tagged LSR, suggesting that LSR is involved in tTJ formation. Furthermore, cellular sheets of two independent LSR-knockdown EpH4 cell clones grown on permeable filters exhibited reduced transepithelial electric resistance (TER) compared with that in normal EpH4 cells, and the lower TER in these cells was mostly recovered by the re-expression of HA–LSR (Fig. 3C), indicating that LSR is also involved in the function of the epithelial barrier.

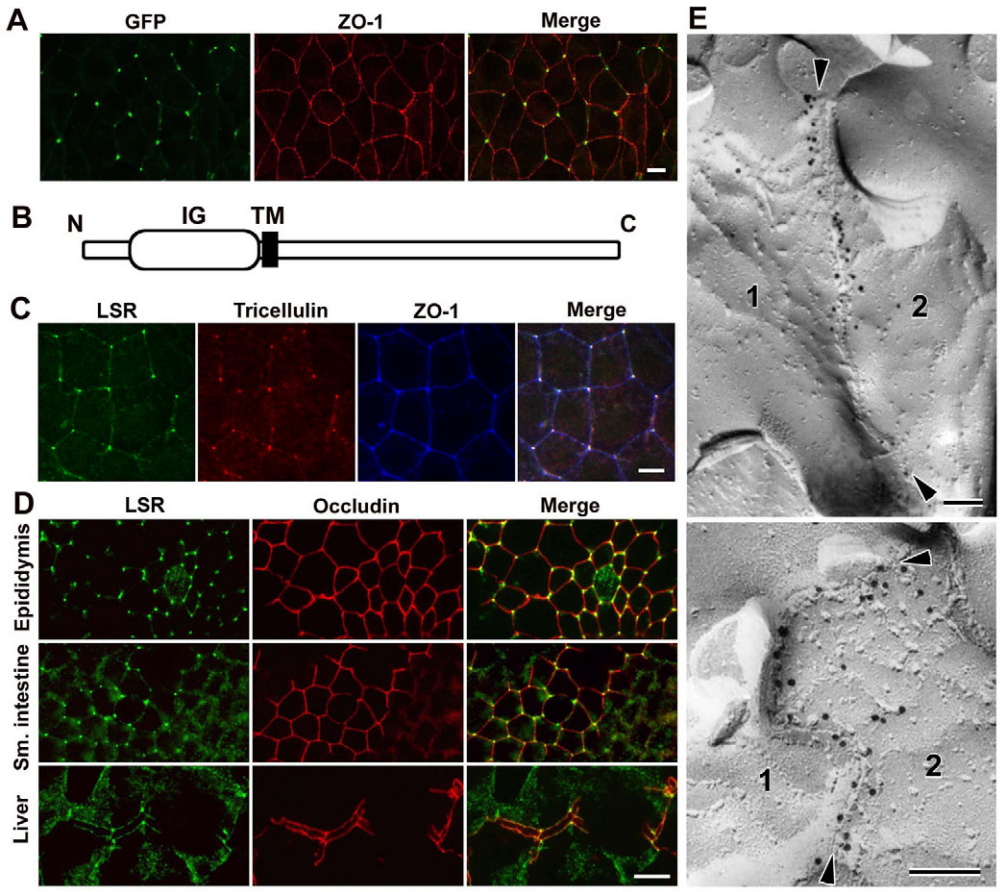

Fig. 1. Identification of LSR as a component of tTJs. (**A**) Localization of a GFP-fusion protein (green) in MDCK cells obtained in an FL-REX screening. Cells were also immunostained with anti-ZO-1 mAb (red) to indicate bTJs. In the merged image, the GFP fusion protein is highly concentrated at tricellular contacts. Three independent experiments showed similar results. A typical experiment had a clear concentration of the GFP fusion protein at 64 of 80 tricellular contacts within 70 cells. Scale bar: 10 µm. (**B**) Structure of LSR. LSR contains an extracellular immunoglobulin domain (IG) and a transmembrane domain (TM). (**C**) Triple immunofluorescence staining of mouse EpH4 cells with anti-LSR pAb (green), anti-tricellulin mAb (red) and anti-ZO-1 mAb (blue). In the merged image, LSR is colocalized with tricellulin at tricellular contacts. Scale bar: 10 µm. (**D**) Double immunofluorescence staining of frozen sections of mouse epididymis, small intestine and liver with anti-LSR pAb (green) and anti-occludin mAb (red). In the liver, the junctional complexes including TJs occur in two parallel lines along bile canaliculi in hepatocytes. The branching points of occludin staining indicate tricellular contacts. In these tissues, LSR is concentrated at tricellular contacts. Weaker signals are also seen at bicellular contacts. In addition, large amounts of LSR are localized at the basolateral membranes in the small intestine and liver. Scale bar: 20 µm. Wide-view images are shown in supplementary material Fig. S1. (**E**) Immuno-freeze-fracture electron microscopy. Freeze-fracture replicas obtained from tricellular contacts of EpH4 cells were immunolabeled with anti-LSR pAb. The central sealing elements (arrowheads) at the center of tTJs between two adjacent cells (1 and 2) are labeled. Scale bars: 200 nm.

Next, we analyzed the relationship between LSR and tricellulin, with regard to their localizations at tTJs (Fig. 3D). Double immunofluorescence staining of the parental EpH4 cells and tricellulin-knockdown cells with the anti-LSR polyclonal antibody and anti-tricellulin monoclonal antibody showed that the tricellular localization of LSR was not affected in tricellulin-knockdown cells. By contrast, the tricellulin accumulation at the tricellular contacts was lost in LSR-knockdown cells. Normal tricellulin accumulation was recovered by re-expression of LSR. Taken together, these observations indicate that LSR recruits tricellulin to tricellular contacts.

The cytoplasmic domain of LSR recruits tricellulin

To determine which domains of LSR are required for its recruitment of tricellulin, we constructed expression vectors for cytoplasmic deletion mutants of LSR tagged with GFP and stably introduced them into LSR-knockdown EpH4 cells. The localization of these GFP–LSR mutants and endogenous tricellulin was then analyzed by immunofluorescence microscopy (Fig. 4). GFP–LSR containing amino acids 1–400 was located at tricellular contacts and recruited tricellulin in a manner similar to full-length LSR. However, GFP-LSR containing amino acids 1–258, although also located at tricellular contacts, was unable to recruit tricellulin. These observations indicate that the cytoplasmic region of LSR is required for its recruitment of tricellulin.

The LSR-mediated recruitment of tricellulin was also reproduced in mouse L fibroblasts. As described previously (Ikenouchi et al., 2008), exogenous HA-tagged full-length tricellulin was distributed throughout the plasma membrane in L cells. By contrast, when introduced into GFP–LSR-expressing L cells, HA-tagged tricellulin colocalized with GFP–LSR (Fig. 5B), demonstrating the recruitment of tricellulin by LSR. Utilizing this system, we further evaluated the roles of the N- and C-terminal cytoplasmic domains of tricellulin in the assembly of tricellulin with LSR (Fig. 5A,B).

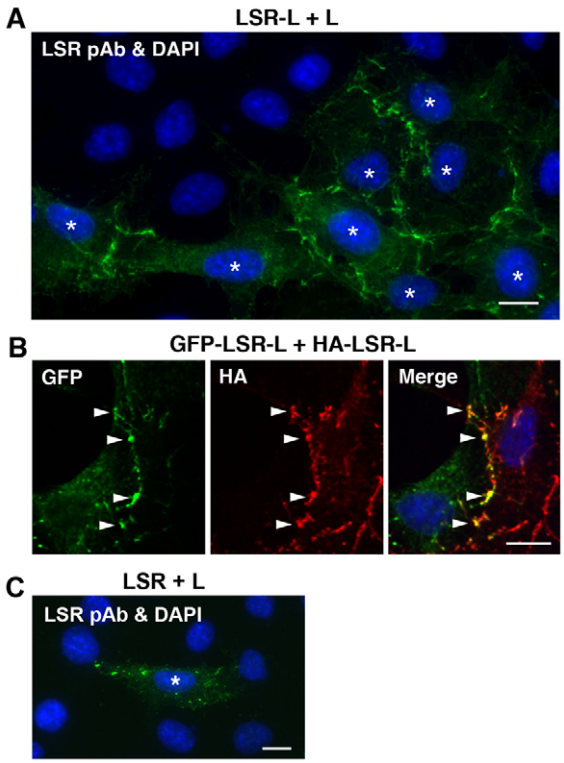

Fig. 2. Assembly of exogenous LSR at cell–cell contacts in mouse L fibroblasts. (**A**) Immunofluorescence staining of co-cultured L cells stably expressing exogenous mouse LSR and parental L cells with anti-LSR pAb (green). The nuclei were co-stained with DAPI (blue). A bright staining intensity for LSR is detected at possible cell–cell contacts between LSR-expressing L cells, whose nuclei are indicated by asterisks. Endogenous LSR is not detected in parental L cells. Scale bar: 10 µm. (**B**) Double immunostaining of co-cultured GFP-tagged LSR-expressing L cells (GFP-LSR-L) and HA-tagged LSR-expressing L cells (HA-LSR-L) with anti-GFP mAb (green) and anti-HA mAb (red). GFP-tagged LSR (green) and HA-tagged LSR (red) are colocalized between GFP–LSR-L cells (left-hand cell) and HA–LSR-L cells (right-hand cell), indicating that LSR assembles at cell–cell contacts. Scale bar: 10 µm. Similar images with a wide-view are shown in supplementary material Fig. S2. (**C**) Immunofluorescence staining of LSR-expressing L cells (asterisk) surrounded by parental L cells with anti-LSR pAb. Accumulation of LSR is detected in single LSR-expressing L cells, although it is unknown whether this occurs at cell–cell contacts. Scale bar: 10 µm. All experiments in A–C were performed three times and similar results were obtained.

When overexpressed in GFP–LSR-expressing L cells, the HA-tagged N-terminal cytoplasmic domain-deleted tricellulin mutant (Tric-ΔN) colocalized with GFP–LSR in a manner similar to full-length tricellulin, whereas the HA-tagged C-terminal cytoplasmic domain-deleted mutant (Tric-ΔC) did not, suggesting that the C-terminal cytoplasmic domain of tricellulin is required for its colocalization with LSR. To confirm this hypothesis, we constructed an expression vector for a chimeric molecule in which the C-terminal cytoplasmic domain of tricellulin was fused to the C-terminus of CD9, a member of the tetraspanin superfamily (Fig. 5A). When introduced into GFP–LSR-expressing L cells, the HA-tagged chimeric molecule (CD9–TricC) was colocalized with GFP–LSR, whereas HA-tagged full-length CD9 was not (Fig. 5C). Consistent with these results, immunoprecipitation experiments using lysates of these cells indicated that HA-tagged CD9–TricC but not CD9 was co-immunoprecipitated with GFP–LSR (Fig. 5D). Taken together, these observations indicate that the recruitment of tricellulin by LSR is mediated by a direct or indirect interaction between the C-terminal cytoplasmic domain of tricellulin and the cytoplasmic domain of LSR.

Discussion

It is not only the cell contacts between two adjacent cells but also tricellular contacts that must be sealed for maintenance of the epithelial barrier. Although the contribution of the latter has been studied less in the field of TJ research, the identification of tricellulin, and the demonstration of its involvement in tTJ formation and in epithelial barrier function, has opened a way to analyze tTJs using molecular cell biological approaches (Ikenouchi et al., 2005). To date, however, the molecular mechanisms behind tTJ formation have mostly remained elusive.

In the present study, we identified LSR as a novel integral membrane protein that is localized at tTJs. RNAi-mediated suppression of LSR expression affected the epithelial barrier function and tTJ formation during cell–cell junction formation. We found that LSR recruited tricellulin to tTJs, suggesting that LSR functions upstream of tricellulin in tTJ formation. On the basis of these observations, a possible model for tTJ formation can be proposed as follows (Fig. 6). LSR assembles at tricellular contacts by an unknown mechanism (discussed below) and generates ‘landmarks’ for tTJ formation. Tricellulin is then recruited to the tricellular contacts through direct or indirect interactions between the cytoplasmic region (amino acids 259–400) of LSR and the C-terminal cytoplasmic domain of tricellulin. Given that tricellulin has an affinity for claudin-based TJ strands within the plasma membrane (Ikenouchi et al., 2005), TJ strands containing tricellulin are recruited to LSR at tricellular contacts to form vertical TJ strands of tTJs. Furthermore, occludin, another TJ-associated membrane protein, excludes tricellulin from bTJs by an unknown mechanism (Ikenouchi et al., 2008), thereby accelerating the accumulation of tricellulin at tTJs. In this model, tricellulin functions as a glue that links claudin-based TJ strands and LSR localized at tricellular contacts. By contrast, when expressed in claudin-1-expressing mouse L fibroblasts in which TJ strands are reconstituted, tricellulin itself can influence the morphology of reconstituted TJ strands by increasing TJ strand crosslinks (Ikenouchi et al., 2008). Indeed, the central sealing elements of tTJs are connected by short TJ strands with crosslinks extended from bTJs (Staehelin, 1973). This notion might imply that tricellulin plays more active roles, rather than just acting as a simple glue. Further investigations are needed to clarify the functions of tricellulin in tTJ formation.

Regarding the interaction between the cytoplasmic domain of LSR and tricellulin, human tricellulin has two splice variants, comprising a longer variant with 558 amino acids, which corresponds to the one we analyzed in mice here, and a shorter variant with 457 amino acids (Schluter et al., 2007). Both variants share amino acids 1–430. Given that the C-terminal cytoplasmic domains of the human tricellulin variants are located between amino acid 364 and the C-terminus, the shorter variant might have different interactions with LSR, thereby showing a localization and function different from the longer variant. However, no splice variants with deletions within the C-terminal cytoplasmic domain of mouse tricellulin are known from public databases.

The most intriguing question for future studies is how LSR becomes localized at tTJs. In L fibroblasts, we observed that LSR

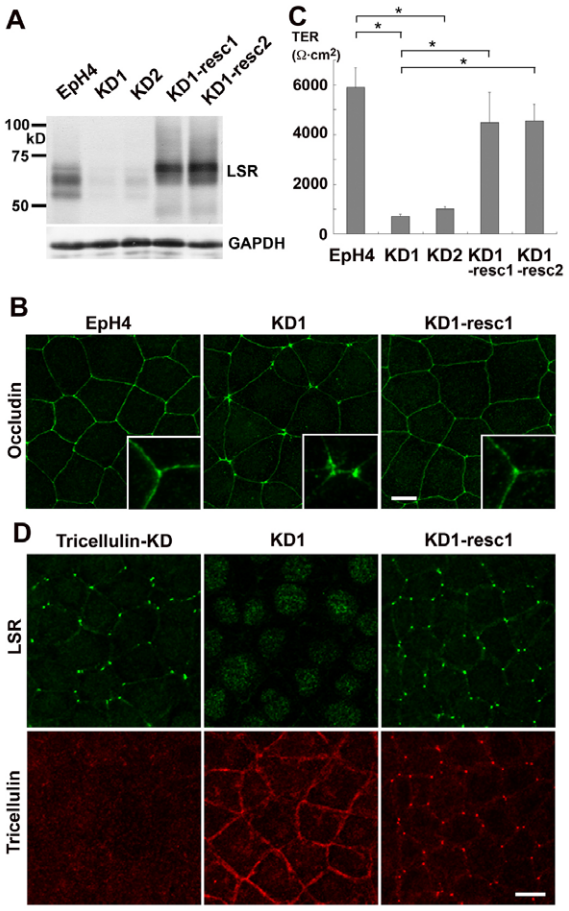

Fig. 3. Stable suppression of LSR expression in EpH4 cells. (**A**) Immunoblot analyses using anti-LSR pAb and anti-GAPDH pAb. Two independent clones with shRNA-mediated stable suppression of LSR expression were established (KD1 and KD2). Next, HA-tagged mouse LSR with silent mutations was introduced into KD1 cells to stably rescue the expression of LSR, and two independent clones (KD1-resc1 and KD1-resc2) were obtained. Equal amounts of total proteins were analyzed by SDS-PAGE and immunoblotting. Note that HA-tagged LSR migrates slightly slower than endogenous LSR, as it contains an additional 34 amino acids, including three HA tags and linkers at the C-terminus. (**B**) Immunofluorescence staining of subconfluent EpH4, KD1 and KD1-resc1 cells with an anti-occludin mAb. Occludin assembly at tricellular contacts is often incomplete in KD1 cells, but this phenotype is rescued in KD1-resc1 cells. Four independent experiments showed similar results. Scale bar: 10 µm. Insets indicate occludin staining at tricellular contacts at a threefold magnification of the main panel. Lower-magnification images from a typical experiment are shown in supplementary material Fig. S3. (**C**) TER measurements of confluent parental EpH4, KD1, KD2, KD1-resc1 and KD1-resc2 cells (n=10 for each cell line). LSR suppression significantly reduces the TER, and this phenotype is rescued by re-expression of HA-tagged LSR. The data are means+s.e.m. *P<0.05. (**D**) Double immunofluorescence staining of tricellulin-knockdown (tricellulin-KD), KD1 and KD1-resc1 cells with anti-LSR pAb (green) and anti-tricellulin mAb (red). Three independent experiments showed similar results. Tricellular localization of LSR is not affected in tricellulin-KD cells. A typical experiment showed that 206 of 210 tricellular contacts within 169 tricellulin-KD cells were LSR positive. In KD1 cells, with suppressed LSR expression, the concentration of tricellulin at tricellular contacts is also diminished. In a typical experiment, no dot-like concentrations of LSR and tricellulin were detected in 162 tricellular contacts within 140 KD1 cells. In KD1-resc1 cells, the concentration of tricellulin at tricellular contacts is recovered by re-expression of HA-tagged LSR. A typical experiment showed that 194 and 192 of 201 tricellular contacts within 152 cells were positive for exogenous HA-tagged LSR and endogenous tricellulin, respectively. Scale bar: 10 µm.

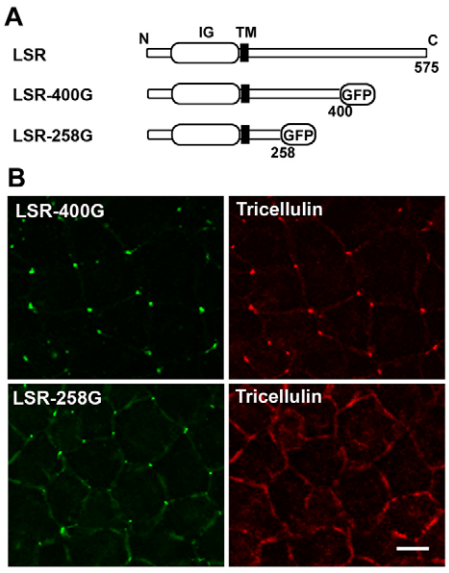

Fig. 4. Introduction of various deletion mutants of LSR into LSR-knockdown EpH4 cells. (**A**) Schematic drawings of the deletion mutants of LSR. The C-terminal cytoplasmic region of mouse LSR was deleted (after amino acid 400 or 258) and GFP tags were linked to the C-termini. The GFP-tagged deletion mutants were designated LSR-400G and LSR-258G, respectively. IG, immunoglobulin domain; TM, transmembrane domain. (**B**) Double immunofluorescence staining of KD1 cells expressing the GFP-tagged LSR deletion mutants with an anti-GFP mAb (green) and an anti-tricellulin mAb (red). Three independent experiments showed similar results. LSR-400G is localized at tricellular contacts together with tricellulin. A typical experiment showed that 125 and 127 of the dot-like concentrations of LSR-400G and tricellulin, respectively, were observed in 127 tricellular contacts within 105 cells. LSR-258G is concentrated at tricellular contacts, but it is unable to recruit tricellulin. A typical experiment showed that 164 of 204 tricellular contacts within 164 cells were positive for LSR-258G, but no dot-like concentrations of tricellulin were observed. Scale bar: 10 µm.

assembled into cell–cell contacts as dots or short lines. This ability of LSR might contribute to its localization in epithelial cells. In addition, there must be unknown mechanisms that control the localization of LSR at tTJs, where three sets of the central sealing elements are bundled (Staehelin, 1973). Given that the deletion mutant of GFP–LSR, containing amino acids 1–258, was accumulated into tricellular contacts, the extracellular region containing an Ig domain, the transmembrane region or the juxtamembrane cytoplasmic region up to amino acid 258 might interact further with unidentified molecules localized at tricellular contacts or recognize unknown biochemical properties of tricellular contacts, such as a specialized cytoskeletal organization or a plasma membrane domain present at epithelial cell corners. Detailed investigations of these domains of LSR, including the search for binding molecules and analyses of biochemical modifications, are ongoing in our laboratory in order to understand the molecular mechanism behind the LSR localization.

The ability to manage cell corners must be one of the fundamental issues for polygonal epithelial cell types, not only for the establishment of the epithelial barrier but also for the maintenance of organized cellular sheets during morphogenesis, when tricellular contacts must be dynamically rearranged, through actomyosin contractility, as cells move relative to each other within the cellular sheet (Fernandez-Gonzalez et al., 2009).

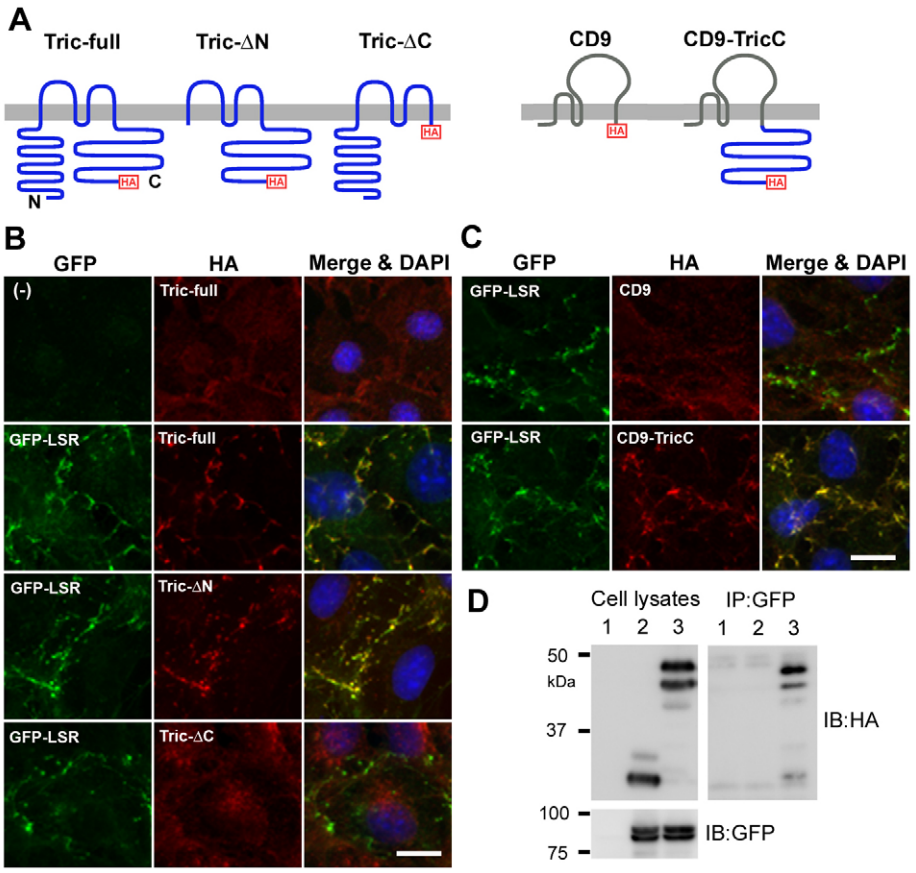

Fig. 5. The domain of tricellulin responsible for its colocalization with LSR. (**A**) Schematic drawings of the various deletion mutants of tricellulin and the chimeric construct used in this study. All the constructs were tagged with HA at their C-termini. Tric-full, full-length tricellulin; Tric-ΔN, N-terminal cytoplasmic domain (amino acids 1–175)-deleted tricellulin; Tric-ΔC, C-terminal cytoplasmic domain (amino acids 396–555)-deleted tricellulin; CD9, full-length CD9; CD9-TricC, chimeric construct of full-length CD9 fused to the C-terminal cytoplasmic domain of tricellulin (amino acids 372–555). (**B**) Double immunofluorescence staining of L cells (–) stably expressing Tric-full, and GFP–LSR L cells stably expressing Tric-full, Tric-ΔN or Tric-ΔC stained with an anti-GFP mAb (green) and anti-HA mAb (red). In the merged images, DAPI-stained nuclei (blue) are also shown. Tric-full and Tric-ΔN are colocalized with GFP–LSR. Scale bar: 10 µm. (**C**) Double immunofluorescence staining of GFP–LSR L cells stably expressing CD9 or CD9–TricC with an anti-GFP mAb (green) and anti-HA mAb (red). In the merged images, DAPI-stained nuclei (blue) are also shown. Note that CD9 but not CD9-TricC is colocalized with GFP–LSR. (**D**) Interaction of the C-terminal cytoplasmic regions of tricellulin and LSR. In the left-hand panel, the expression of CD9, CD9–TricC and GFP–LSR in lysates of L cells (lane 1) and GFP–LSR L cells expressing CD9 (lane 2) or CD9–TricC (lane 3) was analyzed by western blotting with an anti-GFP mAb (IB:GFP) or anti-HA mAb (IB:HA). In the right-hand panel, the cell lysates were subjected to immunoprecipitation (IP) with an anti-GFP mAb, followed by western blotting with anti-HA mAb (IB:HA). CD9–TricC (lane 3), but not CD9 (lane 2), was co-precipitated with GFP–LSR. Wide-view images for B and C are shown in supplementary material Fig. S4.

Another interesting aspect of tricellular contacts is that they are used as ‘windows’ for protrusions from cells just beneath the epithelial cellular sheets, which go out into the lumen to sense the outer environment (Kubo et al., 2009; Shum et al., 2008). They are also possible routes for the transmigration of blood cells and metastatic cancer cells across endothelial cellular sheets (Burns et al., 1997; Nakai et al., 2005). During these processes, how tricellular contact regions are selected and how their open or closed states are regulated remains totally unclear. From this viewpoint, clarification of the whole picture of tTJ formation, including the mechanism for how epithelial cells recognize and generate cell corners, is of great interest as a new research theme in epithelial cell biology.

LSR was originally identified and analyzed as a receptor for the uptake of triacylglyceride-rich lipoproteins (Yen et al., 1999). Previous studies have reported that inactivation of LSR by targeted gene disruption results in embryonic lethality in mice (Mesli et al., 2004) and that heterozygous mice exhibit increased levels of plasma triacylglyceride and cholesterol after food intake (Yen et al., 2008). However, the relationships between the tTJ-associated localization of LSR and its reported functions related to lipoprotein uptake remain totally unknown. These issues should be carefully examined in future studies.

Materials and Methods

Cell culture and transfection

T84 cells were obtained from the American Tissue Culture Collection. EpH4 cells, L cells and MDCKII cells were kind gifts from Ernst Reichmann (University Children’s Hospital Zurich, Zurich, Switzerland), Masatoshi Takeichi (RIKEN CDB, Kobe, Japan) and Masayuki Murata (University of Tokyo, Tokyo, Japan), respectively. All cells were cultured in Dulbecco’s modified Eagle’s medium (DMEM) supplemented with 10% fetal calf serum (FCS). To obtain a uniform EpH4 cell line for experiments, a single-cell clone was obtained by limiting dilution followed by propagation. DNA transfections into EpH4 and L cells were performed using the Lipofectamine Plus reagent (Invitrogen). Tricellulin-knockdown EpH4 cells were established and characterized as described previously (Ikenouchi et al., 2005).

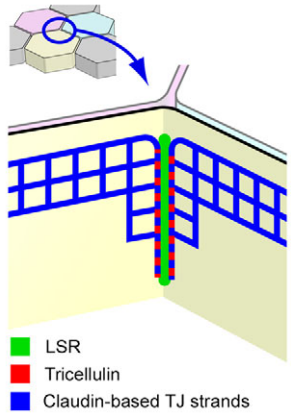

Fig. 6. Model for the organization of tTJs. One tricellular contact is enlarged and viewed from the cytoplasmic side of the yellow cell. See the Discussion section for details.

Antibodies

The rat anti-GFP monoclonal antibody (mAb) and mouse anti-HA mAb (12CA5) were purchased from Roche. The rabbit anti-GAPDH polyclonal antibody (pAb) was purchased from Trevigen. The rat anti-tricellulin mAb (Ikenouchi et al., 2005), rat anti-occludin mAb (Saitou et al., 1998) and mouse anti-ZO-1 mAb (Itoh et al., 1991) were generated and characterized as described previously. The rabbit anti-mouse LSR pAb was raised against a GST fusion protein containing amino acids 361–531 of LSR by Keari (Osaka, Japan). As secondary antibodies for the immunolocalization studies, Alexa-Fluor-488-conjugated donkey anti-(rat IgG) and donkey anti-(rabbit IgG) (Invitrogen), Cy3-conjugated goat anti-(rat IgG) and goat anti-(mouse IgG) (Jackson Immunoresearch Laboratories), Cy5-conjugated goat anti-(mouse IgG) (Jackson Immunoresearch Laboratories) and 10-nm-diameter-gold-labeled goat anti-(rabbit IgG) (AuroProbe; Amersham Biosciences) were used.

Cell screening by FL-REX

A cDNA–GFP fusion library was constructed with polyadenylated RNA isolated from T84 human colonic cancer epithelial cells, using the mouse retrovirus vector pMX, and the cDNA library was then packaged into the high-titer retroviruses using packaging cells, as described previously (Matsuda et al., 2008; Misawa et al., 2000). Visual screening by the FL-REX method (Misawa et al., 2000) was performed as described previously (Matsuda et al., 2008; Nishimura et al., 2002). MDCKII cells expressing virus receptor were infected with the retrovirus library at ~20% infection efficiency. After two days, infected cells were trypsinized, and the GFP-positive cells collected by fluorescence-activated cell sorting (FACS) and sparsely plated onto glass-bottomed dishes. At 48–72 hours after plating, the cells were scanned under an Olympus IX71 fluorescence microscope (Olympus) and cell colonies with a GFP-signal in the cell–cell junctions were marked. At the same time the surrounding colonies were scraped with needles under a phase-contrast microscope and removed by aspiration. After 4–5 days of expansion, the positive colonies were picked up, trypsinized and re-plated onto the glass-bottomed dishes. Cell clones showing the junctional staining were then selected under a fluorescent microscope, picked up in the same way and expanded to prepare their genomic DNAs, which were then used as a template for PCR to recover the integrated cDNA with two primers (5′-GGTGGACCATCCTCTAGACT-3′ and 5′-GTCGCCGTCCAGCTCGAC-3′), followed by direct DNA sequencing.

All the reagents for the generation of the retrovirus-based expression cDNA library were kindly provided by Toshio Kitamura (University of Tokyo, Tokyo, Japan).

cDNA cloning and expression vectors

cDNA encoding the full-length mouse LSR protein was available among the RIKEN FANTOM clones (accession no. AK146807). For further constructs, two *Eco*RI sites within the coding sequence of mouse LSR were disrupted by site-directed mutagenesis without changing the encoded amino acids. To construct LSR-related expression vectors with HA or GFP epitope tags at the C-termini, cDNA fragments encoding full-length or deletion mutants of mouse LSR were amplified by PCR from the mouse LSR cDNA containing the silent mutations and subcloned into pCAGGS-neodelEcoRI (Niwa et al., 1991) with the epitope tag sequences. To construct expression vectors for tricellulin and its deletion mutants, DNA fragments of a mouse tricellulin cDNA (Ikenouchi et al., 2005), as well as its N-terminal or C-terminal deletion mutants generated by PCR, were subcloned into pCAGGSdelneoEcoRI with a C-terminal HA tag. To construct an expression vector for a chimeric protein of CD9 with the C-terminal cytoplasmic region of tricellulin, the C-terminal cytoplasmic region of mouse tricellulin (amino acids 372–555) was generated by PCR and linked to the C-terminus of a monkey CD9 cDNA, kindly provided by Eisuke Mekada (Osaka University, Osaka, Japan), using a conventional molecular cloning technique, and was then subcloned into pCAGGS-neodelEcoRI with a C-terminal HA tag. As a control, an expression vector for HA-tagged CD9 was also generated.

Immunolocalization

Immunofluorescence staining of frozen sections and cultured epithelial cells was performed as described previously (Ikenouchi et al., 2005). For experiments using EpH4 cells or their derivatives, one-thirtieth of confluent cells on a 10-cm-diameter dish were plated onto a 35-mm-diameter dish containing coverslips. The cells on coverslips were used for immunostaining after cultivation for 24 hours (Fig. 3B) or 48 hours (Fig. 1C, Fig. 3D and Fig. 4B). Specimens were embedded in 30% MOWIOL (Calbiochem) and observed with an Olympus IX71 fluorescence photomicroscope. Image acquisition was performed using a combination of an ORCA-ER cooled charge-coupled device camera (Hamamatsu Photonics K.K.) and the IPLab image processing software (BD Biosciences).

Immunoreplica electron microscopy was performed as described previously (Fujimoto, 1995). Eph4 cells were fixed with 1% formaldehyde in 0.1 M phosphate buffer (pH 7.3) for 5 minutes at room temperature, washed three times in 0.1 M phosphate buffer (pH 7.3), immersed in 30% glycerol in 0.1 M phosphate buffer (pH 7.3) for 3 hours and then frozen in liquid nitrogen. The frozen samples were fractured at –100°C and platinum-shadowed unidirectionally at an angle of 45° using a Balzers freeze etching system (BAF060; Bal-Tec). The samples were then immersed in lysis buffer (2.5% SDS, 10 mM Tris-HCl, pH 8.2, and 0.6 M sucrose) and stirred for 12 hours at room temperature. Replicas floating off the samples were washed with PBS containing 5% BSA and processed for immunolabeling with the anti-LSR pAb.

RNAi-mediated suppression of LSR expression and rescue experiments

To suppress the expression of LSR in EpH4 cells, a DNA oligonucleotide (5′-AGAAGAGGCUUUAAAGAAA-3′) against a region of LSR encoding its C-terminus was cloned into an H1 promoter RNAi vector (Brummelkamp et al., 2002). The RNAi construct was transfected into Eph4 cells and confirmed to be effective for suppressing angluin expression.

To express full-length LSR in LSR-knockdown cells, LSR replacement mutants (A1545G, G1548A and T1551C) that did not change the amino acid sequences were generated by site-directed mutagenesis using KOD-plus ver.2 (Toyobo) and *Dpn*I (New England Biolabs).

Measurement of TER

Aliquots containing ~1×10^5 cells were plated onto Transwell filters (12 mm in diameter; six filters for each cell line) and the culture medium was changed daily. The TER was measured directly in culture medium using an epithelial volt–ohm meter (Model Millicell-ERS; Millipore) on day six, when a high-density monolayer had formed. The TER values were calculated by subtracting the background TER, from blank filters, and then multiplying by the surface area of the filter. The data represent the mean and standard error. The statistical significance was evaluated by using Student's *t*-tests.

Immunoprecipitation and western blotting

For immunoprecipitation, cells were solubilized with RIPA buffer containing 1% NP-40, 0.05% SDS, 0.2% sodium deoxycholate, 25 mM HEPES-KOH (pH 7.5), 150 mM NaCl, 1 mM EDTA and 10% glycerol. Cell lysates were treated with an anti-GFP antibody, which was recovered by using protein-G–Sepharose 4 Fast Flow columns (GE Healthcare) and analyzed by SDS-PAGE. All western blotting was performed on Immobilon-P PVDF membranes (Millipore), which were developed using an enhanced chemiluminescence system (GE Healthcare). Blots were scanned with a LAS-3000 mini imaging system (Fujifilm).

This work is dedicated to the memory of Shoichiro Tsukita (deceased 11 December, 2005) who encouraged us to continue the subcellular localization-based screening. We thank T. Kitamura, E. Mekada, E. Reichmann, M. Murata and M. Takeichi for providing reagents and cells, and C. Fujiwara, T. Kato, M. Murata and K. Furuse for their excellent technical assistance. We also thank K. Nagao, M. Amagai, S. Yonemura, A. Nagafuchi and all the members of the Furuse laboratory for helpful discussions. Freeze-fracture electron microscopy was performed in the KAN Research Institute, by courtesy of T. Imai. This study was supported by a Grant-in-Aid for Scientific Research (B) from JSPS, a Grant-in-Aid for Cancer Research, the National Project on Targeted Protein Research Program (TPRP) and the Global COE Program 'Global Center for Education and Research in Integrative Membrane Biology' from the Ministry of Education, Culture, Sports, Science and Technology of Japan, Health and Labor Sciences Research

Grants, and grants from the Cell Science Research Foundation and the Uehara Memorial Foundation (to M.F.).

Supplementary material available online at
http://jcs.biologists.org/cgi/content/full/124/4/548/DC1

References

Angelow, S., Ahlstrom, R. and Yu, A. S. (2008). Biology of claudins. *Am. J. Physiol. Renal Physiol.* **295**, F867-F876.

Brummelkamp, T. R., Bernards, R. and Agami, R. (2002). A system for stable expression of short interfering RNAs in mammalian cells. *Science* **296**, 550-553.

Burns, A. R., Walker, D. C., Brown, E. S., Thurmon, L. T., Bowden, R. A., Keese, C. R., Simon, S. I., Entman, M. L. and Smith, C. W. (1997). Neutrophil transendothelial migration is independent of tight junctions and occurs preferentially at tricellular corners. *J. Immunol.* **159**, 2893-2903.

Farquhar, M. G. and Palade, G. E. (1963). Junctional complexes in various epithelia. *J. Cell Biol.* **17**, 375-412.

Fernandez-Gonzalez, R., Simoes Sde, M., Roper, J. C., Eaton, S. and Zallen, J. A. (2009). Myosin II dynamics are regulated by tension in intercalating cells. *Dev. Cell* **17**, 736-743.

Friend, D. S. and Gilula, N. B. (1972). Variations in tight and gap junctions in mammalian tissues. *J. Cell Biol.* **53**, 758-776.

Fujimoto, K. (1995). Freeze-fracture replica electron microscopy combined with SDS digestion for cytochemical labeling of integral membrane proteins. Application to the immunogold labeling of intercellular junctional complexes. *J. Cell Sci.* **108**, 3443-3449.

Furuse, M. and Tsukita, S. (2006). Claudins in occluding junctions of humans and flies. *Trends Cell Biol.* **16**, 181-188.

Ikenouchi, J., Furuse, M., Furuse, K., Sasaki, H., Tsukita, S. and Tsukita, S. (2005). Tricellulin constitutes a novel barrier at tricellular contacts of epithelial cells. *J. Cell Biol.* **171**, 939-945.

Ikenouchi, J., Sasaki, H., Tsukita, S., Furuse, M. and Tsukita, S. (2008). Loss of occludin affects tricellular localization of tricellulin. *Mol. Biol. Cell* **19**, 4687-4693.

Itoh, M., Yonemura, S., Nagafuchi, A., Tsukita, S. and Tsukita, S. (1991). A 220-kD undercoat-constitutive protein: its specific localization at cadherin-based cell-cell adhesion sites. *J. Cell Biol.* **115**, 1449-1462.

Krug, S. M., Amasheh, S., Richter, J. F., Milatz, S., Gunzel, D., Westphal, J. K., Huber, O., Schulzke, J. D. and Fromm, M. (2009). Tricellulin forms a barrier to macromolecules in tricellular tight junctions without affecting ion permeability. *Mol. Biol. Cell* **20**, 3713-3724.

Kubo, A., Nagao, K., Yokouchi, M., Sasaki, H. and Amagai, M. (2009). External antigen uptake by Langerhans cells with reorganization of epidermal tight junction barriers. *J. Exp. Med.* **206**, 2937-2946.

Li, Y., Fanning, A. S., Anderson, J. M. and Lavie, A. (2005). Structure of the conserved cytoplasmic C-terminal domain of occludin: identification of the ZO-1 binding surface. *J. Mol. Biol.* **352**, 151-164.

Matsuda, M., Kobayashi, Y., Masuda, S., Adachi, M., Watanabe, T., Yamashita, J. K., Nishi, E., Tsukita, S. and Furuse, M. (2008). Identification of adherens junction-associated GTPase activating proteins by the fluorescence localization-based expression cloning. *Exp. Cell Res.* **314**, 939-949.

Mesli, S., Javorschi, S., Berard, A. M., Landry, M., Priddle, H., Kivlichan, D., Smith, A. J., Yen, F. T., Bihain, B. E. and Darmon, M. (2004). Distribution of the lipolysis stimulated receptor in adult and embryonic murine tissues and lethality of LSR–/– embryos at 12.5 to 14.5 days of gestation. *Eur. J. Biochem.* **271**, 3103-3114.

Misawa, K., Nosaka, T., Morita, S., Kaneko, A., Nakahata, T., Asano, S. and Kitamura, T. (2000). A method to identify cDNAs based on localization of green fluorescent protein fusion products. *Proc. Natl. Acad. Sci. USA* **97**, 3062-3066.

Nakai, K., Tanaka, T., Murai, T., Ohguro, N., Tano, Y. and Miyasaka, M. (2005). Invasive human pancreatic carcinoma cells adhere to endothelial tri-cellular corners and increase endothelial permeability. *Cancer Sci.* **96**, 766-773.

Nishimura, M., Kakizaki, M., Ono, Y., Morimoto, K., Takeuchi, M., Inoue, Y., Imai, T. and Takai, Y. (2002). JEAP, a novel component of tight junctions in exocrine cells. *J. Biol. Chem.* **277**, 5583-5587.

Niwa, H., Yamamura, K. and Miyazaki, J. (1991). Efficient selection for high-expression transfectants with a novel eukaryotic vector. *Gene* **108**, 193-199.

Riazuddin, S., Ahmed, Z. M., Fanning, A. S., Lagziel, A., Kitajiri, S., Ramzan, K., Khan, S. N., Chattaraj, P., Friedman, P. L., Anderson, J. M. et al. (2006). Tricellulin is a tight-junction protein necessary for hearing. *Am. J. Hum. Genet.* **79**, 1040-1051.

Saitou, M., Fujimoto, K., Doi, Y., Itoh, M., Fujimoto, T., Furuse, M., Takano, H., Noda, T. and Tsukita, S. (1998). Occludin-deficient embryonic stem cells can differentiate into polarized epithelial cells bearing tight junctions. *J. Cell Biol.* **141**, 397-408.

Schluter, H., Moll, I., Wolburg, H. and Franke, W. W. (2007). The different structures containing tight junction proteins in epidermal and other stratified epithelial cells, including squamous cell metaplasia. *Eur. J. Cell Biol.* **86**, 645-655.

Schneeberger, E. E. and Lynch, R. D. (2004). The tight junction: a multifunctional complex. *Am. J. Physiol. Cell. Physiol.* **286**, C1213-C1228.

Shum, W. W., Da Silva, N., McKee, M., Smith, P. J., Brown, D. and Breton, S. (2008). Transepithelial projections from basal cells are luminal sensors in pseudostratified epithelia. *Cell* **135**, 1108-1117.

Staehelin, L. A. (1973). Further observations on the fine structure of freeze-cleaved tight junctions. *J. Cell Sci.* **13**, 763-786.

Staehelin, L. A., Mukherjee, T. M. and Williams, A. W. (1969). Freeze-etch appearance of the tight junctions in the epithelium of small and large intestine of mice. *Protoplasma* **67**, 165-184.

Van Itallie, C. M. and Anderson, J. M. (2006). Claudins and epithelial paracellular transport. *Annu. Rev. Physiol.* **68**, 403-429.

Wade, J. B. and Karnovsky, M. J. (1974). The structure of the zonula occludens. A single fibril model based on freeze-fracture. *J. Cell Biol.* **60**, 168-180.

Walker, D. C., MacKenzie, A., Hulbert, W. C. and Hogg, J. C. (1985). A re-assessment of the tricellular region of epithelial cell tight junctions in trachea of guinea pig. *Acta Anat. (Basel)* **122**, 35-38.

Yen, F. T., Masson, M., Clossais-Besnard, N., Andre, P., Grosset, J. M., Bougueleret, L., Dumas, J. B., Guerassimenko, O. and Bihain, B. E. (1999). Molecular cloning of a lipolysis-stimulated remnant receptor expressed in the liver. *J. Biol. Chem.* **274**, 13390-13398.

Yen, F. T., Roitel, O., Bonnard, L., Notet, V., Pratte, D., Stenger, C., Magueur, E. and Bihain, B. E. (2008). Lipolysis stimulated lipoprotein receptor: a novel molecular link between hyperlipidemia, weight gain, and atherosclerosis in mice. *J. Biol. Chem.* **283**, 25650-25659.